APL Materials

Efficient methylammonium lead iodide perovskite solar cells with active layers from 300 to 900 nm

Cite as: APL Mater. **2**, 081504 (2014); https://doi.org/10.1063/1.4890056
Submitted: 01 May 2014 • Accepted: 02 July 2014 • Published Online: 16 July 2014

C. Momblona, O. Malinkiewicz, C. Roldán-Carmona, et al.

APL MATERIALS **2**, 081504 (2014)

Efficient methylammonium lead iodide perovskite solar cells with active layers from 300 to 900 nm

C. Momblona,[1] O. Malinkiewicz,[1] C. Roldán-Carmona,[1,2] A. Soriano,[1] L. Gil-Escrig,[1] E. Bandiello,[1] M. Scheepers,[1] E. Edri,[3] and H. J. Bolink[1,a]
[1]*Instituto de Ciencia Molecular, Universidad de Valencia, C/Catedrático J. Beltrán 2, 46980 Paterna, Valencia, Spain*
[2]*Department of Physical Chemistry and Applied Thermodynamics, University of Córdoba, Campus Rabanales, Ed. C3, 14014, Córdoba, Spain*
[3]*Department of Materials and Interfaces, Weizmann Institute of Science, Herzl St. 34, Rehovot 76100, Israel*

(Received 1 May 2014; accepted 2 July 2014; published online 16 July 2014)

Efficient methylammonium lead iodide perovskite-based solar cells have been prepared in which the perovskite layer is sandwiched in between two organic charge transporting layers that block holes and electrons, respectively. This configuration leads to stable and reproducible devices that do not suffer from strong hysteresis effects and when optimized lead to efficiencies close to 15%. The perovskite layer is formed by using a dual-source thermal evaporation method, whereas the organic layers are processed from solution. The dual-source thermal evaporation method leads to smooth films and allows for high precision thickness variations. Devices were prepared with perovskite layer thicknesses ranging from 160 to 900 nm. The short-circuit current observed for these devices increased with increasing perovskite layer thickness. The main parameter that decreases with increasing perovskite layer thickness is the fill factor and as a result optimum device performance is obtained for perovskite layer thickness around 300 nm. However, here we demonstrate that with a slightly oxidized electron blocking layer the fill factor for the solar cells with a perovskite layer thickness of 900 nm increases to the same values as for the devices with thin perovskite layers. As a result the power conversion efficiencies for the cells with 300 and 900 nm are very similar, 12.7% and 12%, respectively. [http://dx.doi.org/10.1063/1.4890056]

Thin film photovoltaic devices hold great promise to reduce the dependencies on fossil energy. Solid state methylammonium lead halide perovskites solar cells are attracting much attention due to their ease of preparation, low cost, and high efficiencies.[1,2] The hybrid organic-inorganic methylammonium lead iodide perovskites have been studied extensively since many years and have been recognized for their excellent semiconducting properties.[3,4] After the seminal work of Miyasaka *et al.*[5] tremendous progress in the performance of methylammonium lead iodide perovskite based solar cells has been obtained.[6–11] Most high efficiency perovskite solar cells reported until now use a (mesoscopic) metal oxide such as Al_2O_3, TiO_2, or ZrO_2 requiring a high temperature sintering process. However, an increasing number of works in which the inverted approach is used are appearing. In these devices, the holes are extracted via the transparent conductor poly(3,4-ethylenedioxythiophene):poly(styrenesulfonic acid) (PEDOT:PSS) situated on top of the transparent bottom electrode.[12–14] Recently, we have improved the performance of such inverted devices by sandwiching an evaporated $CH_3NH_3PbI_3$ perovskite in between organic electron and hole blocking

[a]Author to whom correspondence should be addressed. Electronic mail: henk.bolink@uv.es.

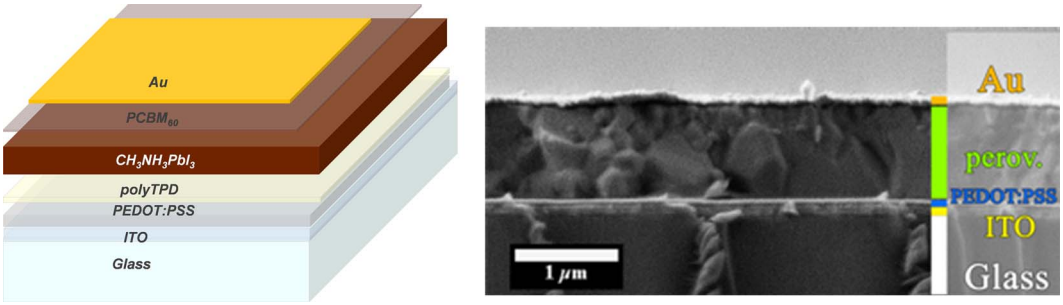

FIG. 1. (a) Schematic presentation of the device layout and (b) SEM cross section image of a device with a perovskite layer thickness of 900 nm. The polyTPD and $PCBM_{60}$ cannot be discerned due to their low thickness.

layers. This configuration leads to stable and reproducible devices that do not suffer from strong hysteresis effects and when optimized lead to efficiencies close to 15%.[15]

Recently, reports have appeared that mention a long charge carrier diffusion length in methylammonium lead iodide perovskite.[16–18] Probably related to that is the observation of a low recombination efficiency of electrons and holes in this material.[19] However, depending on the type of perovskite and its preparation method, very different diffusion lengths, ranging from 100 to 1000 nm, have been reported.

If the longer diffusion lengths hold in real devices one would expect an almost thickness independent performance up to thicknesses equal to the diffusion lengths. To date, most of the perovskite solar cells reported in literature use perovskite layers with thicknesses in the range of 200–400 nm, well below 1 μm. We are aware of only one reference where a thickness dependence study was performed to determine the optimal perovskite layer thickness on PEDOT:PSS on fluorine doped tin oxide (FTO) based glass substrates. From that study, an optimum short-circuit current density (J_{sc}) was found for a perovskite layer thickness of around 450 nm.[20] Additionally, Kelly presented a study on the effect of perovskite thicknesses in a $ZnO/CH_3NH_3PbI_3$/OMTAD device configuration at the HOPV14 conference in Lausanne, he found an optimum J_{sc} for devices having a perovskite thicknesses in the range of 300–400 nm.[21] Both studies used solution processed perovskites layers which are reported to have slightly different properties than vacuum deposited ones. Using our smooth evaporated perovskite films we have prepared perovskite solar cells sandwiched in between organic hole- and electron-blocking layers with perovskite layer thicknesses ranging from 160 to 900 nm. The dual-source thermal evaporation method used to prepare the perovskite layers allows for high precision thickness variations. We show that the J_{sc} of the solar cells increases with increasing perovskite layer thickness, fast up to 300 nm and more slowly for devices with layers going from 300 to 900 nm. However, due to a decreasing fill factor (FF) for cells with perovskite layers in excess of 300 nm the power conversion efficiency (PCE) is reduced for the thicker devices. However, partially oxidation of the poly[N,N′-bis(4-butylphenyl)-N,N′-bis(phenyl)benzidine (polyTPD) electron blocking/hole transporting layer in cells with a 900 nm perovskite layer leads to a recovery of the fill factor and efficiency, reaching similar values as those obtained for the thin perovskite layer based solar cells. This demonstrates that with non-limiting organic layers, the cell performance is rather independent on perovskite layer thickness in between 300 and 900 nm.

The device layout used in this study is shown in Figure 1 and consists of two selective layers situated on both sides of the perovskite layer. To block the electrons and allow holes to reach the anode a thin layer of polyTPD or doped-polyTPD was used. To block holes and allow the electrons to reach the cathode (Au) [6,6]-phenyl C61-butyric acid methylester ($PCBM_{60}$), was used. The indium-tin oxide (ITO) (anode) acts as the hole-collecting contact and the Au (cathode) as the top electron-collecting electrode. Au was selected as it resulted in better performing and more stable devices compared to devices employing other top contact electrodes. A layer of 80 nm of PEDOT:PSS was spin-coated (1200 rpm, 30 s) onto a pre-patterned-ITO containing glass substrate and thermally annealed at 150 °C during 15 min. This layer smoothens the substrate and acts as a hole transporter. Next the polyTPD or doped-polyTPD solution was spin-coated (3000 rpm, 30 s)

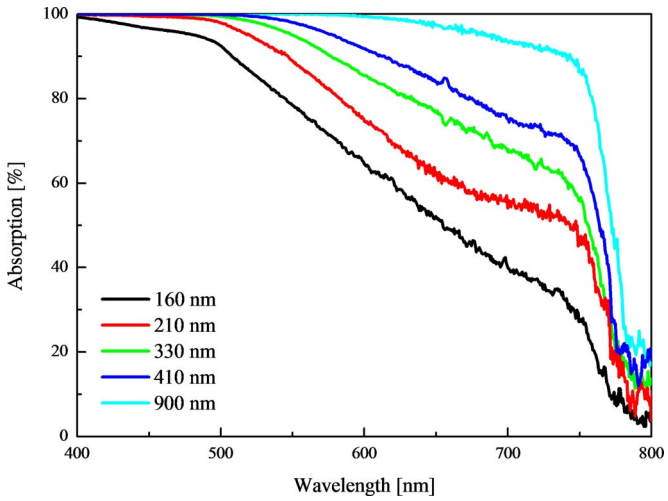

FIG. 2. Absorption spectrum for perovskite thicknesses from 160 to 900 nm.

to obtain a 20 nm thin film. The perovskite was deposited by co-evaporating the two starting materials PbI_2 and CH_3NH_3I in a high vacuum chamber. The thickness of the layers was verified using absorbance and by a stylus profilometer (Ambios X1). Then, a thin layer of 20 nm of $PCBM_{60}$ was deposited using a meniscus coater and a coating speed of 2.5 mm/s.[22] The final stack was covered by 60 nm of Au as the top electrode layer using a vacuum evaporation process. A cross section scanning electron microscopy (SEM) image of a cell with a perovskite layer thickness of 900 nm is shown in Figure 1, where all the layers, except the thin blocking layers, are visible.

The percentage of absorption of the different perovskite layer thicknesses is shown in Figure 2. All films showed an onset of the photocurrent generation at 790 nm, in good agreement with the band gap value (1.55 eV) of the $CH_3NH_3PbI_3$, similar to those reported previously for this material.[23] This broad absorption extends from the visible to the near-IR region. Moreover, the absorption increases almost linearly with the perovskite layer thickness. These spectra were taken on glass substrates, which were also used as the blank. When incorporated into a solar cell, the transmission of the front electrode (ITO) should be taken into account as well as the reflectance at the top Au mirror electrode, which leads to a second pass of the light through the perovskite layer. However, from this figure it is clear that just a single pass of the light through a film with a thickness of 210 nm, leads to more than 50% absorption.

X-ray diffraction analysis of the different thickness perovskite layers is depicted in Fig. S1 of the supplementary material.[24] Slight variations in the diffraction patterns of the different perovskite films are observed. These slight changes are also observed within a series of perovskite layers with a single thickness. Such changes, however, do not lead to large variations of performance as it is evidenced by the narrow statistics that are presented also in Fig. S2 of the supplementary material where an average of 5 to 10 cells are displayed.[24]

As the numbers of photo-generated carriers is related to the number of absorbed photons one expects that J_{sc} increases with increasing layer thickness until all the light is absorbed. With no losses, the remaining parameters, open circuit voltage (V_{oc}) and FF are expected to remain unchanged. Figure 3 summarizes graphically the solar cell performance as a function of perovskite layer thickness. The key performance parameters of the solar cells obtained from the current–density (J) voltage (V) sweeps under 1 sun illumination are plotted versus perovskite layer thickness.

As expected the J_{sc} increases with increasing perovskite layer thickness. It increases rapidly with the perovskite layer thickness from 200 to 300 nm and it continues to increase slowly with further incrementing perovskite layers thickness. Hence, there is still a significant gain in absorption of the sunlight when going from perovskite layers of 200–400 nm. This implies that one cannot simply double the absorption data obtained for a thin film to a device with a mirror top electrode (Fig. 2), but has to take into account the total stack reflectance and absorbance. The increase in J_{sc}

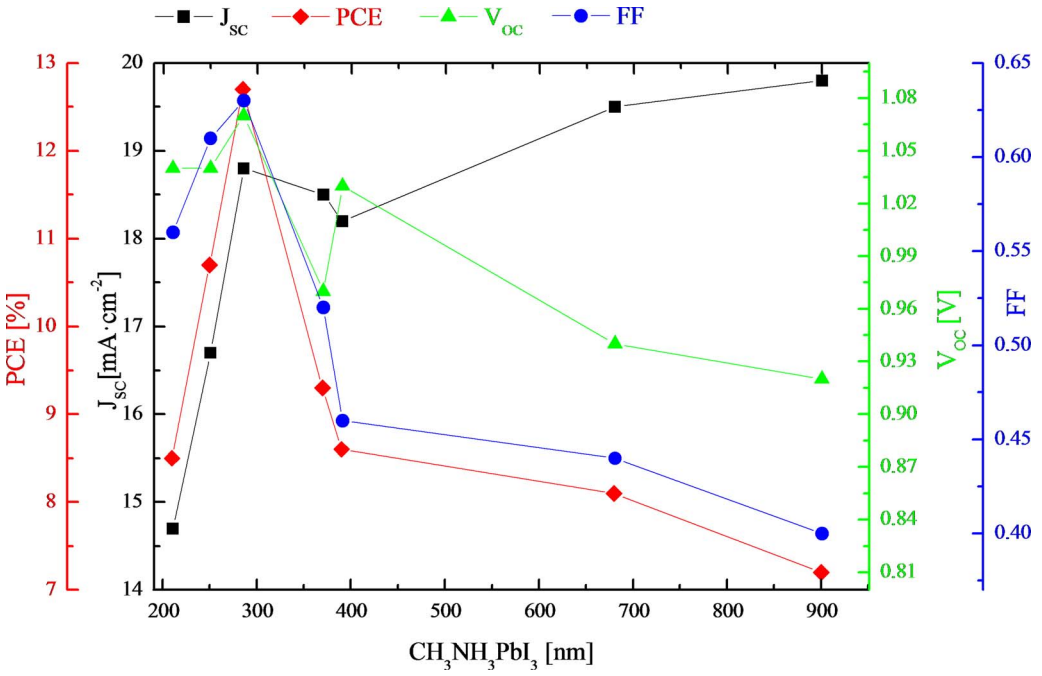

FIG. 3. J_{sc}, V_{OC}, FF, and PCE values as a function of perovskite thickness. For clarity the statistics are not shown in this plot, but are present in the version of this plot in Figure S2 of the supplementary material.[24]

TABLE I. FF values of thick devices at different % of light intensity irradiation.

1 sun intensity [%]	FF
100	48.7
50	52.6
20	55.9
10	58.6
1	63.4

for a device with a perovskite layer of 400 nm to that with a perovskite layer thickness of 900 nm is only around 5%. At the same time, 20% more light is absorbed, and while more free carriers are generated due to increase in light absorbance, the collection efficiency is lower in the thicker device. The V_{oc} is constant for devices with a perovskite layer thickness from 200 to 400 nm. It decreases by nearly 10% for devices with a thicker perovskite layer. The main parameter that is negatively affected by the increase of the perovskite layer thickness is the FF, which drops strongly for devices with a perovskite layer thickness in excess of 300 nm. As a result of the decreasing FF the PCE also decreases with increasing perovskite layer thicknesses. Statistical data is presented in Fig. S2 of the supplementary material.[24]

The decrease in FF is only observed at high light intensity, when this is reduced the FF improves and reaches values similar to the best (thin perovskite layer) devices at 1% of 1 sun (Table I) and Fig S3 of the supplementary material.[24] Hence, with lower charge carrier densities, due to the lower illumination intensity, the FF increases and reaches values similar to what is observed for devices with perovskite layer thickness lower than 300 nm. This implies that the reduction of the fill factor is not primarily related to the increased path length for the charge carriers, i.e., series resistance in the absorber layer. Yet it appears to be related to the efficiency of charge extraction. This can be due to, e.g., the lower hole mobilites in the polyTPD compared to that of holes in the perovskite layers, and can also be related to smaller built in voltage in the thicker devices. From previous work on

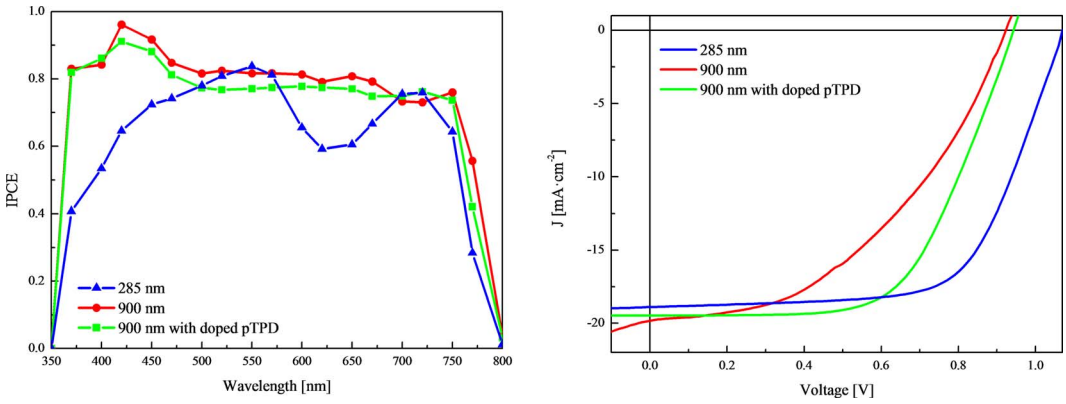

FIG. 4. (a) IPCE curves and (b) photocurrent density versus voltage under 1 sun illumination, for a thin, a thick, and a thick device with doped hole transporting layer.

organic light-emitting diodes (OLEDs) it is known that the conductivity of the polyTPD increases superlinearly when it is partially oxidized (doped).[25] Yet, high doping levels may hamper the layer's ability to block electrons, therefore, for this study we replaced the pristine polyTPD with a slightly oxidized version polyTPD (0.05% oxidized). Using this doped electron blocking/hole transporting layer solar cells were prepared with perovskite layer thickness of 900 nm (Fig. 4).

With this partially oxidized polyTPD layer the FF of the solar cells at 1 sun light intensity is recovered and reaches values similar of the devices with perovskite layers up to 400 nm (Table II). The V_{oc} seems not to be affected by the doping of the polyTPD and remains almost the same as with the undoped thick cell (slightly below 1 V). Due to the slightly higher J_{sc}, the slightly lower V_{oc} and similar FF, the PCE of the solar cells with perovskite layer thicknesses of 285 and 900 nm reaches 12.7% and 12.0%, respectively. This is yet another example of the high electronic quality of organic-inorganic lead halide perovskite materials. It can be attributed to the large charge carrier diffusion lengths observed in solution processed $CH_3NH_3PbI_3$ perovskite. As mentioned in these studies the observed diffusion lengths depend on the preparation method, therefore, it is possible that in evaporated $CH_3NH_3PbI_3$ perovskite layer even larger diffusion length of charge carriers are present. The effect of the doped polyTPD layer on cells employing a thinner perovskite layer was negligible (Fig. S4 of the supplementary material).[24]

Our device architecture employing PEDOT:PSS and ITO as the anode and Au as the cathode, the built-in potential is expected to be small in view of the small off set in work functions of these two electrodes (5.0 and 5.1 eV, respectively). However, it is known that the interactions of metals and organics can change the effective work functions. This built-in potential assists in the separation of electrons to one direction and holes to the opposite one. Using capacitance voltage scans an estimate of the flat band potential around 1 V was obtained, confirming the presence of a built-in potential (Fig. S5 of the supplementary material).[24] Following the p-i-n model suggested to describe how these devices work, increasing the doping in the selective contacts leads to an increase in the built-in potential in the absorber. This can explain the large difference in FF between low and high light intensities for the thick devices: at low light intensity, most of the built in potential is still present leading to high FF; at high light intensities the bands are flatter and hence the lower FF. This will not be so in thin devices as the electric field is larger (the potential difference being the same, yet the layer being thinner). Another support for this hypothesis we find in the dark J-V of the various devices (Fig. S6 of the supplementary material), where the diode onset is shifted to higher voltages when the polyTPD in the thick device is doped.[24] Our results demonstrate that the solar cell performance is high over a wide range of thicknesses (300–900 nm) simplifying large area processing requirements, hence facilitating industrial production scales.

To conclude, methylammonium lead iodide perovskite solar cells have been prepared with a wide range of active layer thicknesses. With undoped hole transport layers the best performances are obtained for solar cells with a perovskite layer thickness around 300 nm, reaching a PCE of 12.7%

TABLE II. Current density–voltage data of ITO/PEDOT:PSS/polyTPD/$CH_3NH_3PbI_3$/$PCBM_{60}$/Au at different perovskite thicknesses.

$CH_3NH_3PbI_3$ [nm]	J_{SC} [mA/cm^2]	V_{OC} [V]	FF [%]	PCE [%]
210	14.7	1.04	0.56	8.6
250	16.7	1.04	0.61	10.6
285	18.8	1.07	0.63	12.7
370	18.5	0.97	0.52	9.3
390	18.2	1.03	0.46	8.6
680	19.5	0.94	0.44	8.1
900	19.8	0.92	0.4	7.2
900[a]	19.5	0.94	0.65	12.0

[a]This device corresponds to ITO/ PEDOT:PSS/doped-polyTPD (0.05% $AgSbF_6$)/$CH_3NH_3PbI_3$/$PCBM_{60}$/Au configuration.

in this series. However, if the hole transport materials is slightly doped by adding a small amount of an oxidant to it, the solar cell performance is almost independent on perovskite layer thickness. For a device with a perovskite layer thickness of 900 nm, a PCE of 12% was obtained only slightly below that of the best device with a perovskite layer thickness of 300 nm. These results demonstrate that the carriers generated in this layer do not suffer from recombination losses even in such very thick layers, corroborating earlier reports of long carrier diffusion lengths.

All chemicals and solvents used were obtained from Sigma-Aldrich and used as received unless stated otherwise. ITO covered glass substrates were purchased from NaranjoSubstrates. PEDOT:PSS CLEVIOS P VP Al 4083 was purchased from Hereaus Holding and used as received. Poly[N,N′-bis(4-butylphenyl)-N,N′-bis(phenyl)benzidine (polyTPD) was purchased from American Dye Source and [6,6]-phenyl C61-butyric acid methylester ($PCBM_{60}$) from Solenne B.V. Both of them were used as received. For their application they were dissolved in chlorobenzene solutions (7 mg ml^{-1} and 10 mg ml^{-1}, respectively). Doped-poly(TPD) corresponds to 7 mg ml^{-1} of polyTPD with a 0.05 molar% in $AgSbF_6$ purchased from Sigma-Aldrich. Solutions were freshly prepared before using. PbI_2 was purchased from Sigma-Aldrich and CH_3NH_3I was synthesized following the procedure previously reported.[26] In short, CH_3NH_3I was synthesized by reacting 26 ml of methylamine (40 wt.% in water) and 10 ml of hydroiodic acid (57 wt.% in water) in a 250 ml round-bottomed flask at 0 °C for 2 h under magnetic stirring. The white precipitate was recovered by evaporation at 50 °C for 1 h. The product was dissolved in ethanol, filtered and recrystallized from diethyl ether and dried at 70 °C in an oven for 24 h. Fresh CH_3NH_3I was synthesized before each set of experiments. Perovskite was synthetized using a vacuum chamber of MBraun integrated in an inert glovebox (MBraun). The starting materials were placed in ceramic crucibles which were heated up from two evaporation sources from Creaphys. The substrates were placed at 20 cm from the top of the ceramic crucibles. A shutter was present below the substrate holder, being closed until the adequate PbI_2/CH_3NH_3I ratio was achieved. At a pressure of 1×10^{-6} mbar, CH_3NH_3I was heated to 70 °C. Once the sensor reading was stable, PbI_2 was heated until 250 °C to obtain dark brown perovskite layers. The process was followed by three quartz microbalance sensors placed in the chamber. Typically 4 cells of 0.06 cm^2 are present on each substrate. Up to 5 substrates can be coated with the perovskite in one single co-evaporation step.

All the characterizations, except the UV-Vis absorption spectra and profilometer measurements, were done in a nitrogen filled glove box (<0.01 ppm O_2 and <0.1 ppm H_2O) without exposure to ambient. Absorption measurements were done using a fibre-optics based Aventes Avaspec 2048 spectrometer. J-V curves were recorded in a MiniSun simulator by ECN the Netherlands. During the measurements, the devices were illuminated by a white light halogen lamp and using a mask overlaying the sample which only illuminated the active area of the cells. Before each measurement, the exact light intensity was determined using a calibrated Si reference diode equipped with an infrared cut-off filter (KG-3, Schott). An estimation of the short-circuit current density (J_{sc}) under standard test conditions was calculated by convolving the external quantum efficiency (EQE) spectrum with the AM1.5G reference spectrum, using the premise of a linear dependence of J_{sc} on light intensity.

Current-voltage (J-V) curves were measured using a Keithley 2400 source measure unit. The scan was performed with steps of 0.01 V starting from −0.2 V to 1.1 V with a time delay between each point set to 0.01 s. The perovskite films were characterized by using grazing incidence X-ray diffraction (GIXRD) after its evaporation. The measurements were done at room temperature in the 2θ range 5º–50º on an Empyrean PAN analytical powder diffractometer, using Cu Kαl radiation. The capacitance-voltage measurements were performed using a Keithley 4200-SCS parameter analyzer. Voltage sweeps were performed with a step of 0.05 V in the range from −0.8 to +0.8 V (33 points for each sweep). The capacitance values were obtained by measuring the impedance of the samples at 1 KHz frequency and with an applied ac voltage of 10 mV rms. During the measurements, the samples were kept inside a Faraday cage, to screen them from external electromagnetic interferences.

This work was supported by the Spanish Ministry of Economy and Competitiveness (MINECO) (MAT2011-24594), the Generalitat Valenciana (Prometeo/2012/053). E.B. acknowledges MINECO for an FPI grant. C.R.-C. would like to thank the MINECO for the financial support of this research in the framework of project CTQ2010-17481, the Junta de Andalucía (CICyE) for special financial support (P10-FQM-6703), and the MECD (Spanish Ministry of Education, Culture, and Sport) for a FPU grant.

[1] P. Gao, M. Gratzel and M. K. Nazeeruddin, "Organohalide lead perovskites for photovoltaic applications," Energy Environ. Sci. (published online).
[2] H. J. Snaith, J. Phys. Chem. Lett. **4**(21), 3623–3630 (2013).
[3] C. R. Kagan, D. B. Mitzi, and C. D. Dimitrakopoulos, Science **286**(5441), 945–947 (1999).
[4] A. Poglitsch and D. Weber, J. Chem. Phys. **87**(11), 6373–6378 (1987).
[5] A. Kojima, K. Teshima, Y. Shirai, and T. Miyasaka, J. Am. Chem. Soc. **131**(17), 6050–6051 (2009).
[6] M. M. Lee, J. Teuscher, T. Miyasaka, T. N. Murakami, and H. J. Snaith, Science **338**(6107), 643–647 (2012).
[7] J. M. Ball, M. M. Lee, A. Hey, and H. J. Snaith, Energy Environ. Sci. **6**(6), 1739–1743 (2013).
[8] J. Burschka, N. Pellet, S.-J. Moon, R. Humphry-Baker, P. Gao, M. K. Nazeeruddin, and M. Gratzel, Nature (London) **499**(7458), 316–319 (2013).
[9] M. Liu, M. B. Johnston, and H. J. Snaith, Nature (London) **501**(7467), 395–398 (2013).
[10] O. Malinkiewicz, A. Yella, Y. H. Lee, G. M. Espallargas, M. Graetzel, M. K. Nazeeruddin, and H. J. Bolink, Nat. Photon **8**(2), 128–132 (2014).
[11] D. Liu and T. L. Kelly, Nat. Photon **8**(2), 133–138 (2014).
[12] J.-Y. Jeng, Y.-F. Chiang, M.-H. Lee, S.-R. Peng, T.-F. Guo, P. Chen, and T.-C. Wen, Adv. Mater. **25**(27), 3727–3732 (2013).
[13] S. Sun, T. Salim, N. Mathews, M. Duchamp, C. Boothroyd, G. Xing, T. C. Sum, and Y. M. Lam, Energy Environ. Sci. **7**(1), 399–407 (2014).
[14] Q. Wang, Y. Shao, Q. Dong, Z. Xiao, Y. Yuan, and J. Huang, Energy Environ. Sci. **7**, 2359–2365 (2014).
[15] O. Malinkiewicz, C. Roldán, A. Soriano, E. Bandiello, L. Camacho, M. K. Nazeeruddin, and H. J. Bolink, Adv. Energy Mater. **4**, 1400345 (2014).
[16] G. Xing, N. Mathews, S. Sun, S. S. Lim, Y. M. Lam, M. Grätzel, S. Mhaisalkar, and T. C. Sum, Science **342**(6156), 344–347 (2013).
[17] S. D. Stranks, G. E. Eperon, G. Grancini, C. Menelaou, M. J. P. Alcocer, T. Leijtens, L. M. Herz, A. Petrozza, and H. J. Snaith, Science **342**(6156), 341–344 (2013).
[18] E. Edri, S. Kirmayer, A. Henning, S. Mukhopadhyay, K. Gartsman, Y. Rosenwaks, G. Hodes, and D. Cahen, Nano Lett. **14**(2), 1000–1004 (2014).
[19] C. Wehrenfennig, G. E. Eperon, M. B. Johnston, H. J. Snaith, and L. M. Herz, Adv. Mater. **26**(10), 1584–1589 (2014).
[20] P. Docampo, J. M. Ball, M. Darwich, G. E. Eperon, and H. J. Snaith, Nat. Commun. **4**, 2761 (2013).
[21] T. Kelly, in proceedings of the HOPV14 conference, Lausanne, 2014.
[22] O. Malinkiewicz, M. Lenes, H. Brine, and H. J. Bolink, RSC Adv. **2**(8), 3335–3339 (2012).
[23] T. Baikie, Y. Fang, J. M. Kadro, M. Schreyer, F. Wei, S. G. Mhaisalkar, M. Graetzel, and T. J. White, J. Mater. Chem. A **1**(18), 5628–5641 (2013).
[24] See supplementary material at http://dx.doi.org/10.1063/1.4890056 for additional information such as x-ray, J-V data, and C-V data.
[25] S. Cheylan, J. Puigdollers, H. J. Bolink, E. Coronado, C. Voz, R. Alcubilla, and G. Badenes, J. Appl. Phys. **103**(9), 096110 (2008).
[26] L. Etgar, P. Gao, Z. Xue, Q. Peng, A. K. Chandiran, B. Liu, M. K. Nazeeruddin, and M. Grätzel, J. Am. Chem. Soc. **134**(42), 17396–17399 (2012).